Smart Drug Delivery

Deutsche Ausgabe: DOI: 10.1002/ange.201505437
Internationale Ausgabe: DOI: 10.1002/anie.201505437

Protein Delivery System Containing a Nickel-Immobilized Polymer for Multimerization of Affinity-Purified His-Tagged Proteins Enhances Cytosolic Transfer

*Viktoriia Postupalenko, Dominique Desplancq, Igor Orlov, Youri Arntz, Danièle Spehner, Yves Mely, Bruno P. Klaholz, Patrick Schultz, Etienne Weiss, and Guy Zuber**

Abstract: *Recombinant proteins with cytosolic or nuclear activities are emerging as tools for interfering with cellular functions. Because such tools rely on vehicles for crossing the plasma membrane we developed a protein delivery system consisting in the assembly of pyridylthiourea-grafted polyethylenimine (πPEI) with affinity-purified His-tagged proteins pre-organized onto a nickel-immobilized polymeric guide. The guide was prepared by functionalization of an ornithine polymer with nitrilotriacetic acid groups and shown to bind several His-tagged proteins. Superstructures were visualized by electron and atomic force microscopy using 2 nm His-tagged gold nanoparticles as probes. The whole system efficiently carried the green fluorescent protein, single-chain antibodies or caspase 3, into the cytosol of living cells. Transduction of the protease caspase 3 induced apoptosis in two cancer cell lines, demonstrating that this new protein delivery method could be used to interfere with cellular functions.*

More than 60 recombinant proteins and monoclonal antibodies (mAbs) are available for treatment of human pathologies.[1] Proteins are generally membrane-impermeable, a property that constrains their use as pharmaceutical products to extracellular targets.[2] It is estimated that membrane-associated or secreted proteins account for about 30% of the protein coding capacity of a genome,[3] leaving the remaining 70% of putative targets unreachable. To explore intracellular targets, it is crucial to develop methods for transferring proteins inside cells. One approach uses associative interactions between the protein and a synthetic cationic carrier to build supramolecular delivery systems.[4] However, electrostatic associations between the carrier and proteins are not always strong enough for assembly of effective delivery systems because the number of anionic side-chain residues per protein is limited and varies from one protein to another.[4b] One solution for reducing the influence of protein charge variation on the protein/carrier assembly is to covalently modify the protein with negatively charged macromolecules.[5] Here, we propose to attach several proteins onto a polyanionic linear guide (pGi) using reversible non-covalent association. Electrostatic interactions between the pGi-bound proteins and a cationic carrier such as the pyridylthiourea-grafted polyethylenimine (πPEI)[6] may then be exploited for building the delivery system (Figure 1).

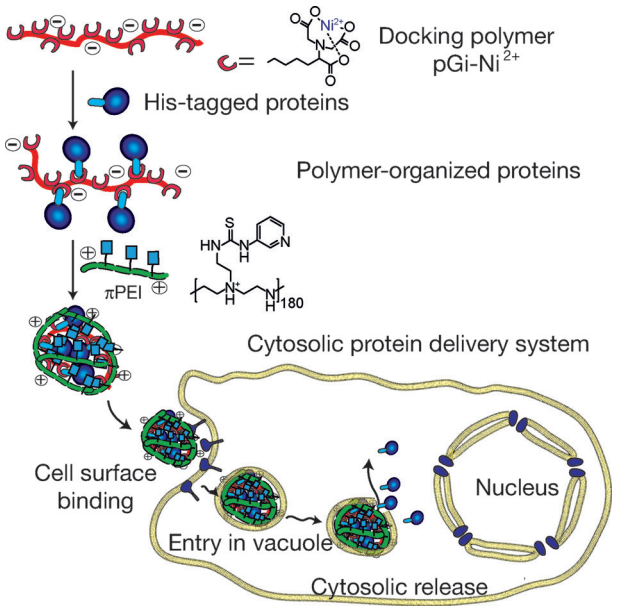

Figure 1. Illustration of the protein delivery system. His-tagged proteins are docked onto a Ni^{2+}-immobilized polymer. The docked proteins are then packed with the πPEI carrier for cytosol transfer using the cell vesicular machinery.

For protein immobilization, selective coordination of histidine (His) by nitrilotriacetic acid (NTA)-immobilized divalent nickel (Ni^{2+}), with a K_D in the 1–10 μM range,[7] seems a perfect match. First, it constitutes a popular affinity chromatography method and affords a potential large library of purified His-tagged proteins.[8] Secondly, NTA is anionic and it can favor electrostatic cohesion with a cationic carrier. Thirdly, even mild acidic conditions (pH 6.0) weaken the association between the protein and the Ni^{2+}–NTA group. This may allow release in PEI-buffered intracellular vacuoles.[6] Finally, NTA-chelated[9] or soluble nickel ions[10]

[*] Dr. V. Postupalenko, Dr. Y. Arntz, Dr. Y. Mely, Dr. G. Zuber
UMR 7199 and UMR 7213 CNRS Université de Strasbourg
Faculté de Pharmacie, Illkirch (France)
E-mail: zuber@unistra.fr
Dr. D. Desplancq, Dr. E. Weiss
UMR 7242, Ecole supérieure de biotechnologie Strasbourg
Illkirch (France)
Dr. I. Orlov, Dr. D. Spehner, Dr. B. P. Klaholz, Dr. P. Schultz
Centre for Integrative Biology (CBI), IGBMC
Illkirch (France)

Supporting information for this article is available on the WWW under http://dx.doi.org/10.1002/anie.201505437.

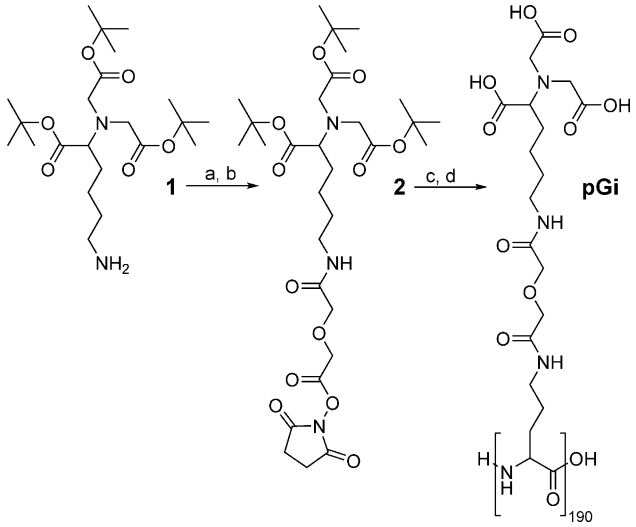

Scheme 1. Synthesis of pGi. a) Diglycolic anhydride, 4-dimethylaminopyridine (DMAP), CH_2Cl_2. b) *N*,*N*′-dicyclohexylcarbodiimide, N-hydroxysuccinimide. c) Polyornithine, DMAP, dimethylformamide/water. d) Trifluoroacetic acid.

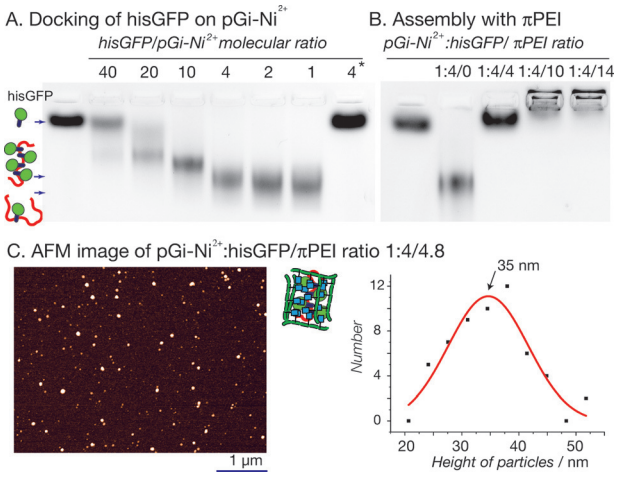

Figure 2. HisGFP association to pGi-Ni^{2+} and to πPEI carrier. A) Electrophoretic mobility of hisGFP alone (first lane) and with increasing amounts of pGi-Ni^{2+}. *In the last lane, the complex was mixed with EDTA. B) Mobility of [pGi-Ni^{2+}:hisGFP] following association with πPEI. C) AFM image of hisGFP-containing delivery complex and size distribution.

can be administrated in vivo at doses that do not induce observable adverse effects in rodent.

The pGi was prepared according to Scheme 1. The carboxylate-protected NTA **1**[11] was reacted with diglycolic anhydride. The dangling carboxylic acid was activated to a succinimidyl ester **2**, which was coupled to polyornithine. Unreacted cationic amines were converted to carboxylic acid by reaction with diglycolic anhydride and protecting groups were removed with trifluoroacetic acid. Extensive dialysis yielded pGi, a polymer grafted with approximately 150 NTA groups as estimated by NMR spectroscopy. Ni^{2+} was then immobilized on pGi and provided pGi-Ni^{2+} to an estimated Ni immobilization on 50% of the NTA groups.

The docking capacity of pGi-Ni^{2+} was evaluated by mixing the polymer with 75 equivalents of a fluorescently labeled 1.6 kDa hexahistidine-containing peptide (one peptide per immobilized nickel ion). The free peptides were then separated from the polymer-bound ones in an ultrafiltration device, allowing determination of a maximum docking of 20 peptides per polymer. Repetition of this experiment with His-tagged green fluorescent protein (hisGFP, 29 kDa) yielded a lower docking capacity of 10 proteins per polymer. The bulkiness of the protein, which presumably covers two times more NTAs than the peptide, explains these different capacities. The effect of stoichiometry on the association was analyzed by monitoring the variation in hisGFP electrophoretic mobility within an agarose gel (Figure 2 A).

The hisGFP alone (lane 1) migrated in the gel as a single band. Addition of pGi-Ni^{2+} modified the protein mobility towards a faster moving band in a dose-dependent manner. A band with an electrophoretic mobility similar to that of hisGFP alone was observed when the nickel ion bridging the hisGFP and the polymer were displaced with EDTA (last lane). Association between [pGi-Ni^{2+}:hisGFP] and πPEI was similarly assayed (Figure 2 B). Four hisGFPs were docked per pGi-Ni^{2+} and the cationic πPEI was added in increasing amounts. A complete association was achieved at a πPEI/hisGFP ratio of 2.5. Atomic force microscopy (AFM) of [pGi-Ni^{2+}:hisGFP/πPEI] at a ratio 1:4/4.8 showed a distribution of round-shaped particles with a mean height of 35 nm (Figure 2 C).

Insight into how His-tagged molecules associate onto the linear pGi-Ni^{2+} at maximum docking capacity was next explored by AFM and cryo-electron microscopy (cryo-EM). The hisGFP alone or bound to pGi-Ni^{2+} were seen only using cryo-EM as individual dots or serpentine filaments, respectively (Figure S1). For finer resolution and confirmation, we aimed at substituting the soft and low contrasting protein with a harder and higher contrasting material. The 2 nm-diameter mercaptobenzoic acid-coated gold nanocluster was selected because it has a molecular weight of 28 kDa similar to hisGFP, is easily prepared in large quantities and its surface may be functionalized through exchange of mercaptobenzoic acid with thiolated biomolecules.[12] The gold clusters were prepared and reacted with a thiolated hexahistidine-containing peptide to afford the His-tagged gold nanoclusters (hisAuNC). We verified that they formed a fully dispersed colloidal solution and associated with pGi-Ni^{2+} similarly to His-tagged proteins (Figures S2 and S3). The hisAuNC were docked onto pGi-Ni^{2+} at the maximum docking capacity of the polymer (measured as 12 hisAuNC per pGi-Ni^{2+}) and unbound hisAuNC were removed by dialysis for AFM and cryo-EM analyses (Figure 3 A).

The purified [pGi-Ni^{2+}:$(hisAuNC)_{12}$] were seen as filamentous assemblies composed of distinct 2 nm particles. In the diluted EM condition, about 10 to 20 distinct dots were seen to cluster and roughly align in oblong superstructures, corresponding presumably to single or dimeric [pGi-Ni^{2+}:hisAuNC]. These observations confirmed the gel mobility assays and demonstrated the ability of the linear polymer to bind and congregate His-tagged materials. The purified [pGi-Ni^{2+}:$(hisAuNC)_{12}$] was then mixed with πPEI (final ratio

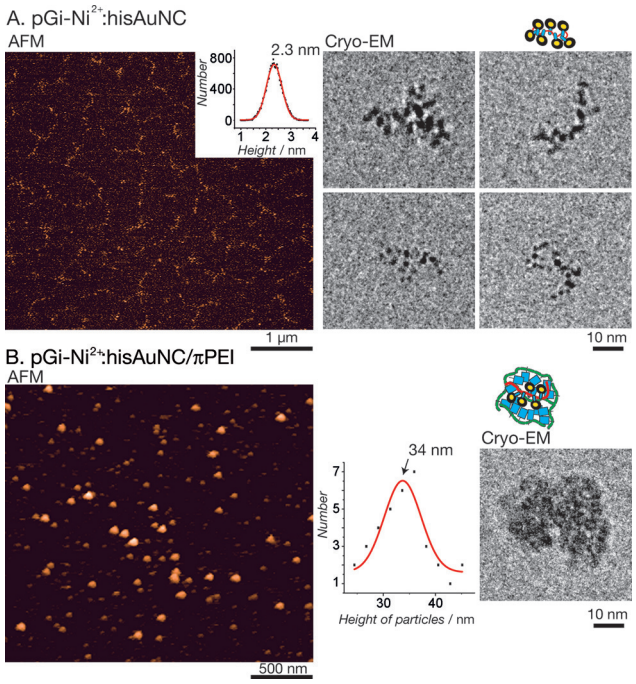

Figure 3. Atomic force and cryo-electron micrographs of supramolecular assemblies incorporating His-tagged gold nanoclusters (hisAuNC). A) [pGi-Ni^{2+}:hisAuNC], ratio 1:12. B) [pGi-Ni^{2+}:hisAuNC/πPEI], ratio 1:12/14.4.

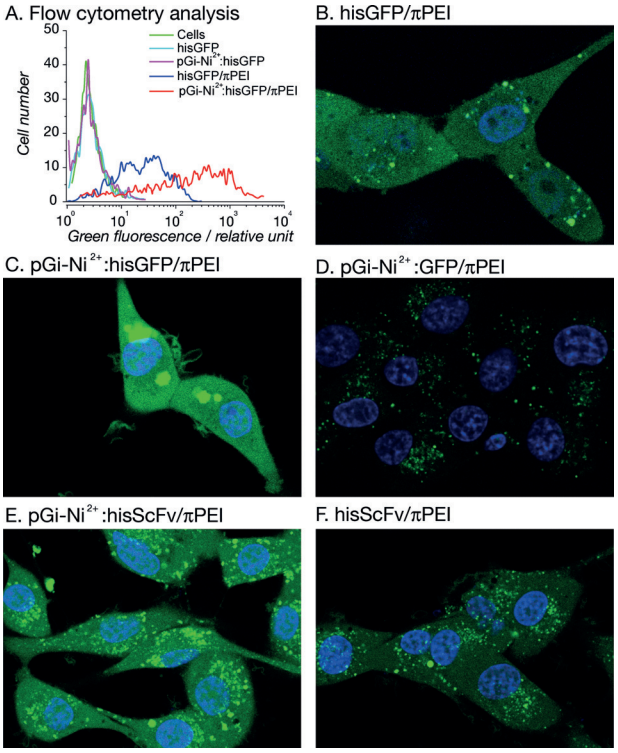

Figure 4. πPEI and pGi-assisted cytosolic delivery of hisGFP and Alexa488-labeled hisScFv in living U87 cells (24 h incubation). The cell nuclei were stained (blue) with Hoechst 33242. The pGi-Ni^{2+}:hisprotein/πPEI input molar stoichiometries were 0:4/9.6 or 1:4/4.8. In image D, the GFP was without a His-tag. Protein concentrations were of 120 nM.

1:12/14.4) and observed again by AFM and cryo-EM (Figure 3B). With both methods, the ternary assembly displayed a spherical shape with a mean height/diameter of 34 nm similarly to the hisGFP-containing vehicle (Figure 2C) and to [hisAuNC/πPEI] (Figure S4). Individual gold particles or filaments were not apparent within the polyplex likely because the AuNC were buried and closely packed within the soft shell of πPEI.

The delivery property of the assemblies was next evaluated in U87 glioblastoma cells using an easily detectable fluorescent protein (Figure 4). The ability of various assemblies to associate with U87 cells was first quantified by flow cytometry (Figure 4A). As shown, the hisGFP alone or [pGi-Ni^{2+}:hisGFP] did not associate with the cells (no modification of the green fluorescence signal by comparison to untreated cells), whereas [hisGFP/πPEI] or [pGi-Ni^{2+}:hisGFP/πPEI] did (Figure 4A). The pGi-Ni^{2+} containing vehicle yielded on average a ten-fold enhancement of the green fluorescence intensity as compared with the same vehicle lacking it. Important to note, a pGi-Ni^{2+}:hisprotein/πPEI molar ratio of 1:4/4.8 consistently yielded optimal cellular delivery. Four his-tagged proteins per pGi-Ni^{2+} is 2.5 times smaller than the maximum docking capacity of the polymer. This sub-maximal binding condition allows partial multimerization and enhanced polyplex cohesiveness by complementary electrostatic association between πPEI and unmasked anionic NTA domains surrounding the proteins. The described protein delivery system had a similar size distribution and colloidal stability in cell culture medium regardless of the protein or presence of pGi (Figures S5 and S6). These data suggest that the pGi-mediated enhanced intracellular protein delivery yield is due to increased inflow of polyplexes and not to entry of larger polyplexes containing more protein.

The localization of delivered proteins within living cells was next tracked by fluorescence microscopy. The cells incubated with [hisGFP/πPEI] contained fluorescent aggregates, presumed to be hisGFP remaining entrapped within vesicular compartments but also a diffuse green fluorescence in the cell interior, signifying cytosolic release (Figure 4B). A similar cell fluorescence distribution was observed using [pGi-Ni^{2+}:hisGFP/πPEI] polyplexes but with an enhanced cytosolic fluorescence intensity (Figure 4C). We attempted to deliver GFP without its His-tag in which case it did not bind to pGi-Ni^{2+} (Figure S7). Result showed that cellular uptake of these polyplexes was poor (Figure 4D), demonstrating the importance of his-tagged protein binding to pGi-Ni^{2+} in the enhanced efficiency. We then delivered his-tagged recombinant antibody fragments since such proteins may be therapeutic alternatives for full-length antibodies. The anti-tubulin single-chain variable fragment 2G4 was previously characterized.[13] It was labeled with Alexa488 (hisScFv), docked on the pGi-Ni^{2+}, and packed with πPEI. The delivery system was added to U87 cells, and the living cells were observed (Figure 4E). A delivery pattern similar to that of hisGFP was observed. The absence of microtubule staining may appear puzzling but was already noticed for the delivery of an anti-tubulin IgG inside the cytosol of living cell.[14] We suspect that excess unbound hisScFvs masked the micro-

tubule staining. Again, the cytosolic, diffuse green fluorescence was brighter for cells treated with the pGi-Ni^{2+}-containing system (Figure 4E) than the one without it (Figure 4F).

We finally delivered a bioactive protein. The cytosolic protease caspase 3 participates in a signaling pathway leading to cell apoptosis and may find applications in cancer therapy by inducing tumor cells to undergo programed cell death.[15] A commercially available His-tagged caspase 3 (hiscasp) was assembled onto pGi-Ni^{2+} and entrapped with πPEI. The vehicle was then incubated with U87 cells for 24 h and cell viability was quantified by assaying for succinate dehydrogenase activity (Figure 5). All of the control conditions, consisting of incubation of the cells either with hiscasp alone, [pGi-Ni^{2+}:hiscasp], [hisGFP/πPEI] or [pGi-Ni^{2+}:hisGFP/πPEI], did not significantly alter the cell viability. In contrast, [hiscasp/πPEI] and the fully organized [pGi-Ni^{2+}:hiscasp/πPEI] led to statistically significant 40 and 80% decreases in cell viability, respectively. The apoptotic event was confirmed by visualization of condensed nuclei in the [pGi-Ni^{2+}:hiscasp/πPEI] treated cells (Figure S8). The entire [pGi-Ni^{2+}:hiscasp/πPEI] system proved most efficient in assisting caspase-3-mediated cytotoxicity when added onto Hela cells (Figure S9).

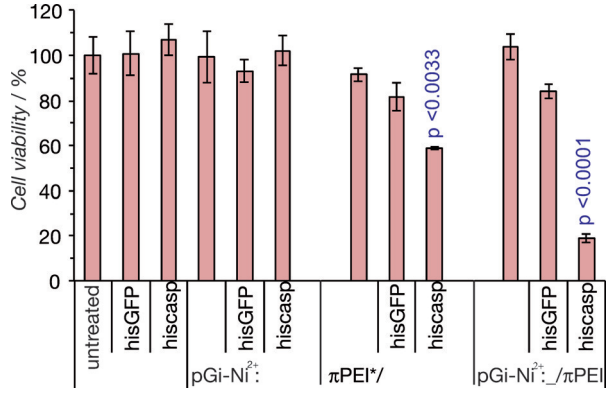

Figure 5. Delivery of His-tagged caspase 3 (hiscasp) and hisGFP into U87 cells. Cells were incubated for 24 h and the mean cell viability was plotted relative to untreated cells. Concentrations were 20 nM pGi-Ni^{2+}, 80 nM protein, and 96 (or *192) nM πPEI.

In summary, we report a strategy for cytosolic protein delivery compatible with current methodologies of protein preparation. It is based on the reversible and specific assembly of His-tagged proteins onto a soluble nickel-immobilized polymer, followed by packaging with a cationic carrier. This pre-organizing step enhanced biological activity and cytosolic transfer for various His-tagged proteins. We believe that the protein delivery system reported here is efficient enough to be assayed in cancer therapy applications particularly when topical administration is an option.

Acknowledgements

We are grateful to R. Drillien for discussions. This work was supported by grants from the ANR Chromact, FRISBI (grant numbers ANR-10-INSB-05-01, ANR-10-LABX-0026_CSC) and Instruct ESFRI.

Keywords: drug delivery · nanocarriers · protein delivery · proteins · self-assembly

How to cite: *Angew. Chem. Int. Ed.* **2015**, *54*, 10583–10586
Angew. Chem. **2015**, *127*, 10729–10732

[1] J. G. Elvin, R. G. Couston, C. F. van der Walle, *Int. J. Pharm.* **2013**, *440*, 83–98.
[2] J. P. da Cunha, et al., *Proc. Natl. Acad. Sci. USA* **2009**, *106*, 16752–16757.
[3] M. Diehn, R. Bhattacharya, D. Botstein, P. O. Brown, *PLoS Genet.* **2006**, *2*, e11.
[4] a) A. Fu, R. Tang, J. Hardie, M. E. Farkas, V. M. Rotello, *Bioconjugate Chem.* **2014**, *25*, 1602–1608; b) L. Kurzawa, M. Pellerano, M. C. Morris, *Biochim. Biophys. Acta Biomembr.* **2010**, *1798*, 2274–2285.
[5] a) A. A. Eltoukhy, D. Chen, O. Veiseh, J. M. Pelet, H. Yin, Y. Dong, D. G. Anderson, *Biomaterials* **2014**, *35*, 6454–6461; b) Y. Lee, T. Ishii, H. J. Kim, N. Nishiyama, Y. Hayakawa, K. Itaka, K. Kataoka, *Angew. Chem. Int. Ed.* **2010**, *49*, 2552–2555; *Angew. Chem.* **2010**, *122*, 2606–2609.
[6] a) S. Pinel, E. Aman, F. Erblang, J. Dietrich, B. Frisch, J. Sirman, A. Kichler, A. P. Sibler, M. Dontenwill, F. Schaffner, G. Zuber, *J. Controlled Release* **2014**, *182*, 1–12; b) V. Postupalenko, A. P. Sibler, D. Desplancq, Y. Nomine, D. Spehner, P. Schultz, E. Weiss, G. Zuber, *J. Controlled Release* **2014**, *178*, 86–94.
[7] L. Nieba, S. E. Nieba-Axmann, A. Persson, M. Hamalainen, F. Edebratt, A. Hansson, J. Lidholm, K. Magnusson, A. F. Karlsson, A. Pluckthun, *Anal. Biochem.* **1997**, *252*, 217–228.
[8] a) J. Porath, J. Carlsson, I. Olsson, G. Belfrage, *Nature* **1975**, *258*, 598–599; b) H. Block, B. Maertens, A. Spriestersbach, N. Brinker, J. Kubicek, R. Fabis, J. Labahn, F. Schafer in *Guide to Protein Purification*, *Vol. 463*, 2nd ed. (Eds.: R. R. Burgess, M. P. Deutscher), Elsevier Academic Press, San Diego, **2009**, pp. 439–473.
[9] V. Platt, Z. Huang, L. Cao, M. Tiffany, K. Riviere, F. C. Szoka, Jr., *Bioconjugate Chem.* **2010**, *21*, 892–902.
[10] L. T. Haber, G. L. Diamond, Q. Zhao, L. Erdreich, M. L. Dourson, *Regul. Toxicol. Pharmacol.* **2000**, *31*, 231–241.
[11] S. Lata, A. Reichel, R. Brock, R. Tampe, J. Piehler, *J. Am. Chem. Soc.* **2005**, *127*, 10205–10215.
[12] A. A. Sousa, J. T. Morgan, P. H. Brown, A. Adams, M. P. Jayasekara, G. Zhang, C. J. Ackerson, M. J. Kruhlak, R. D. Leapman, *Small* **2012**, *8*, 2277–2286.
[13] P. Philibert, A. Stoessel, W. Wang, A. P. Sibler, N. Bec, C. Larroque, J. G. Saven, J. Courtete, E. Weiss, P. Martineau, *BMC Biotechnol.* **2007**, *7*, 81.
[14] D. Dalkara, G. Zuber, J. P. Behr, *Mol. Ther.* **2004**, *9*, 964–969.
[15] K. Yamabe, S. Shimizu, T. Ito, Y. Yoshioka, M. Nomura, M. Narita, I. Saito, Y. Kanegae, H. Matsuda, *Gene Ther.* **1999**, *6*, 1952–1959.

Received: June 13, 2015
Published online: July 31, 2015

